

MEAN CRYSTALLITE SIZE, SIZE DISTRIBUTION AND ROOT MEAN SQUARE RESIDUAL MICROSTRAIN MEASUREMENT FROM X-RAY LINE BROADENING

Modern X-ray techniques, methods and limits



M. Dănilă

e-mail: mihaid@imt.ro

National Institute for R&D in Microtechnologies, P.O.Box 38-160, Bucharest, Romania,
<http://www.imt.ro>,

One of the simplest available ways of producing nano-structured materials (i.e. nano-powders) is the milling (grinding) technique. However, producing nano-powders with a crystallite size down to ten nanometers is a very daunting task. In this application-oriented study, we have investigated the structural changes of commercially available ZnSe powders induced by the milling process. Those changes were revealed by the wide angle X-ray diffraction technique using the X-ray line broadening ('direct', Stokes Fourier method, Hall-Williamson and Warren-Averbach method). We found that the initial powder had a crystallite size $D \sim 90\text{nm}$ (Scherrer equation) and a micro-strain $\epsilon = \Delta d/d \sim 10^{-5}$. After 40 hours of grinding the ZnSe powder had a crystallite size D of 12-14 nm and $\epsilon \sim 3.9 \cdot 10^{-3}$. The nanopowders obtained by the grinding technique can thus be used in photonic and opto-electrical applications.

Experimental

The initial powder was found to be the FCC ZnSe cubic phase (stilleite), fully crystalline with no strain. The initial powder had a very low content (<1%) of ZnO (zincite). The X-ray spectra of the initial powder ($t=0\text{h}$) was used as reference to produce measures of line broadening of the milled samples. Mean crystallite size D , size distribution and r.m.s. residual strain ϵ were computed from them. The milling was carried in a centrifugal ball mill, Retsch S100, with 20mm diameter agatha balls for 2.5, 3.5, 5, 7.5, 10, 20 and 40 h. The X ray spectra were recorded by the wide-angle X-ray diffraction method (θ - 2θ coupling, λ CuK α , fig. 1-2). The diffraction lines were deconvolved for overlapping, instrumental broadening and microstructure of the samples using the Lorentz, Gauss and Pearson VII fitting functions. The unfolded pattern is used then to perform the classical plotting methods (fig.3) [2]. The full width at half maximum $\beta_{1/2}$ was chosen as the measure for the X-ray line broadening.

Results

The X-ray spectra were processed using the program CRYSiZ, developed at the Oak Ridge National Laboratory, USA (Hall-Williamson analysis, Stokes Fourier coefficient method and Warren-Averbach analysis- fig.4,5) [4].

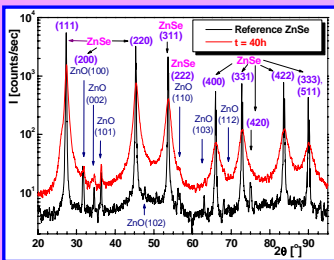


Fig. 1. X-ray spectrae ($t = 0\text{h}$, $t = 40\text{h}$)

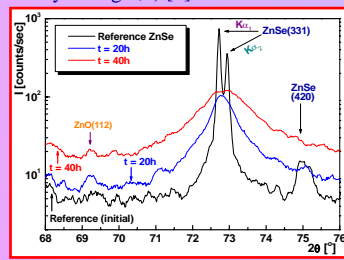


Fig. 2. Detail of fig.1 : (331) peak

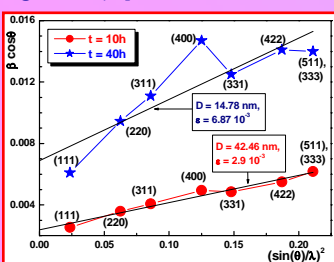


Fig.3. Hall-Williamson Cauchy-Gauss plot using FWHM (Gauss fit)

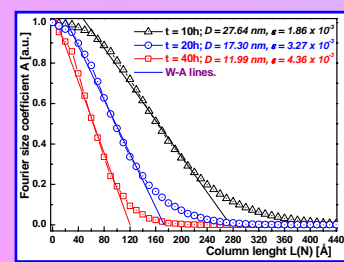


Fig.4. Warren-Averbach size coefficient all lines (Cauchy-Gauss, Gauss fit)

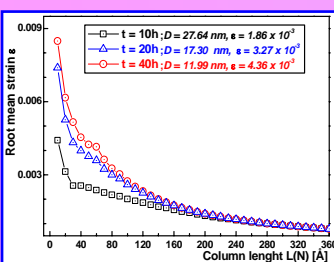


Fig.5. Warren-Averbach strain distribution (Cauchy-Gauss, Gauss fit)

The results of this work (derived from Hall Williamson method - fig.1 and Warren-Averbach method - fig.3,4) are presented in tables 1,2. Strain values are stable, less sensitive to the deconvolution model (fig.6 to 10). The Warren-Averbach method produces size and strain values smaller than those predicted by the plotting methods. After 40 h of milling some amorphous ZnSe phase develops, together with a reduction of the crystallite size D to a nanometer scale and an increase of the microstrain ($D=12\text{nm}$, $\epsilon = 6 \cdot 10^{-3}$). It is interesting to note that ZnO crystallites keep a constant size value of 12~14nm.

Acknowledgements

The author is greatly indebted to dr. R.Peascoe Meissner (Ohio State University) and dr. C.Hubbard (ORNL) who kindly offer the Fortran source code used here.

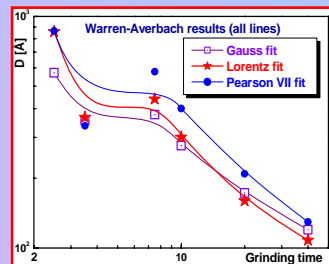


Fig.6. Warren-Averbach size values

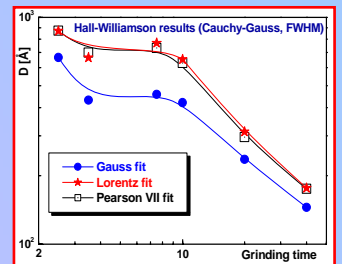


Fig.7. Hall-Williamson size values

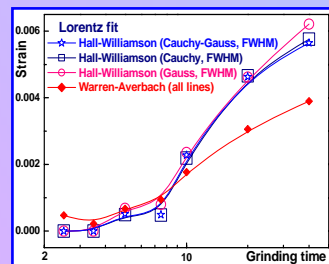


Fig.8. Strain evolution (Lorentz fit)

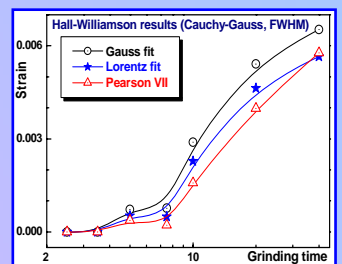


Fig.9. Strain evolution (H-W)

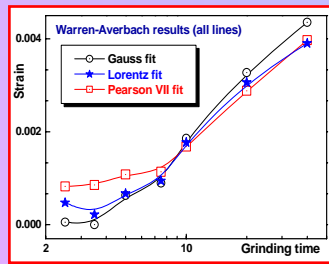


Fig.10. Strain evolution (WA2)

Single Bragg lines focusing <ul style="list-style-type: none"> Quantitative and qualitative phase analysis Crystal structure analysis of powders Percent crystallinity analysis Crystallite size/lattice strain analysis 	
Parallel beams <ul style="list-style-type: none"> Phase and structure analysis of thin films and powders Lattice parameter refinement Texture and stress analysis Thin thickness, density, and roughness analysis 	
2-D Bragg mosaic <ul style="list-style-type: none"> Structure analysis of imperfect crystals Orientation analysis of oriented films Phase and orientation identification of oriented films, density, and roughness analysis Thin thickness, density, and roughness analysis 	
High resolution triple-axis <ul style="list-style-type: none"> Structure analysis of highly perfect crystals Orientation analysis of highly perfect oriented films Crystal quality analysis of highly perfect crystal substrates Thin thickness, density, and roughness analysis 	
In-plane geometry <ul style="list-style-type: none"> Phase and structure analysis of ultra thin films Depth controlled phase identification Depth controlled structure analysis Texture analysis of thin films 	

Supported powder diffraction applications include: <ul style="list-style-type: none"> Phase identification Quantitative analysis Percent crystallinity Crystallite size/lattice strain analysis Precise lattice parameter determination Retrieval refinement 	SAXS applications include: <ul style="list-style-type: none"> Particle size distributions of nanoparticles suspended in solution Particle size distributions in dispersed or bulk solid nanomaterials Particle shape analysis Correlation function analysis of irregular electron density distributions 	
	<ul style="list-style-type: none"> Composition Orientation/texture Perfection Relaxation Strain/stress 	
	<ul style="list-style-type: none"> Thickness Interface roughness Density Surface uniformity 	

References

- [1] G.Williamson, W.Hall, Acta Metallurgica, vol Lpp 22-31
- [2] N.Durand et al, J. Phys. France 4(1994) 1025-1032.
- [3] Y.Rosenberg et al, J.Phys.Cond.Matt.12 (2000),8081-8088.
- [4] ORNL/TM-13273, C.R.Hubbard,B.R. Morosin,J.M.Stewart, 1996, contract no. DE-AC05-90OR2264 and T01. DE-AC04-94AL85000 (at Sandia National Laboratories) managed by Lockheed Martin Energy Research Corp. for the US Dept. of Energy, Oak Ridge National Laboratory, Metals and Ceramics Division, Oak Ridge Tennessee, USA.